Ocean Modelling 29 (2009) 223–233

Contents lists available at ScienceDirect

Ocean Modelling

journal homepage: www.elsevier.com/locate/ocemod

Cluster synchronisation: A mechanism for plankton patchiness and a simulation pitfall

Emma Guirey [a,*], Adrian Martin [a], Meric Srokosz [a], Martin Bees [b]

[a] National Oceanography Centre, Southampton, SO14 3ZH, UK
[b] Department of Mathematics, University Gardens, University of Glasgow, G12 8QW, UK

ARTICLE INFO

Article history:
Received 11 December 2008
Received in revised form 16 April 2009
Accepted 24 April 2009
Available online 8 May 2009

Keywords:
Plankton patchiness
Synchronisation theory
Metapopulation
Biophysical modelling

ABSTRACT

We present a study on the emergence of spatial variability, or patchiness, in biophysical simulations of plankton ecosystems. Using a standard approach to modelling such ecosystems, we represent a distribution of plankton as a lattice of non-identical interacting oscillatory populations. Spatial variation is imposed in population parameters, such as maximum growth rate, leading to a spread in the natural (uncoupled) population properties. Using the methods of synchronisation theory, the emergent spatial structure of the coupled system is investigated as a function of the strength of interaction between populations. Surprisingly, a range of coupling strength is found to induce a tenfold increase in the spread in frequency of oscillation of populations in comparison with the uncoupled level of spatial variation. This apparent desynchronisation corresponds to the formation of temporally evolving clusters of local synchronisation: the interplay of grid-cell scale variability and dispersal between populations leads to patchiness at larger scales. However, the occurrence and length-scale of this patchiness is found to be sensitive to typical simulation parameters such as spatial resolution and strength of dispersal, with emergent spatial structure altering abruptly from patchy to homogeneous as these parameters are varied. These results indicate that whilst cluster synchronisation may be a genuine mechanism for the formation of spatial structure in plankton distributions, biophysical modellers should be aware of the possibility of artificial patchiness arising from the basic physical structure of their model.

1. Introduction

In this study, we use the methods of synchronisation theory to explore how the emergence of plankton patchiness in biophysical models of the surface ocean is influenced by the underlying model assumptions and structure.

The distribution of plankton in the ocean is spatially and temporally heterogeneous with "patchiness" on scales of centimetres to several hundred kilometres. This is a well-known phenomenon that has been observed for many years from ships (see e.g. Bainbridge, 1956) and, more recently, by satellite. Patchiness and its consequences are not fully described or understood, and the importance of plankton cannot be denied: plankton are significant players in the carbon cycle and form the base of most marine foodwebs. Patchiness in plankton distributions has been linked with levels of primary productivity and the stability and persistence of a population (Steele, 1974). For example, in their study of freshwater protists, Holyoak and Lawler (1996) found that a patchy population has a reduced risk of extinction, since migration between interacting patches allows recolonisation of depleted patches. Since current Global Carbon Cycle Models that are used in global and regional modelling are incapable of resolving features of the mesoscale and smaller (Fasham, 2003), the scale at which much of the variability in plankton distribution is seen (Steele, 1978), they may be incurring large errors. A better understanding of heterogeneity in real-world and modelled plankton dynamics may therefore improve our ability to model, understand and predict carbon cycle dynamics.

A typical approach to modelling plankton ecosystems is to discretise the region into spatial grid-cells with the physical flow represented as interactions between grid-cells. The biological dynamics in each grid-cell, assuming well-mixed dynamics, is represented by a plankton ecosystem model which attempts to break down the complicated structure of a marine ecosystem into a number of components (zooplankton, phytoplankton, detritus, etc.) and the interactions between them. The coupled biophysical model can then be used to investigate and predict observed features of plankton distributions and production (e.g. Levy and Klein, 2004; Abraham, 1998).

This type of system is the concern of synchronisation theory, which studies how the natural rhythms of time-varying entities adjust as a result of coupling between them (Pikovsky et al., 2001).

* Corresponding author. Present address: Scottish Government, Marine Laboratory, P.O. Box 101, 375 Victoria Road, Aberdeen, AB11 9DB, UK. Tel.: +44 12 2429 5439.
E-mail addresses: e.j.guirey@marlab.ac.uk (E. Guirey), apm1@noc.soton.ac.uk (A. Martin), mas@noc.soton.ac.uk (M. Srokosz), m.bees@maths.gla.ac.uk (M. Bees).

1463-5003/$ - see front matter © 2009 Elsevier Ltd. All rights reserved.
doi:10.1016/j.ocemod.2009.04.006

Examples of synchronised dynamics in systems of interacting oscillators have been found in all areas of science including electronics (e.g. Taherion and Lai, 1999; Neff and Carroll, 1993), biology (e.g. Strogatz and Stewart, 1993), epidemiology (e.g. Boccaletti, 2002), lasers (e.g. Barbay et al., 2000) and human behaviour (e.g. Néda et al., 2000). If the interaction between oscillators causes their states to become uniform in time, then the system is *fully synchronised*. Alternatively, the frequencies or phases of the oscillators may become synchronised whilst the amplitudes remain uncorrelated. In addition, instead of synchrony occurring across the whole ensemble, the system may break up into subgroups of (fully/phase/frequency, etc.) synchronised oscillators, with no synchrony between subgroups. This is referred to as *cluster synchronisation* (Osipov and Sushchik, 1997; Belykh et al., 2003; Pascual et al., 2002). Spatially synchronised fluctuations in population sizes across large distances have been documented for wide variety of species including rodents (Sherratt et al., 2000; Ydenberg, 1987; Haydon et al., 2001), birds (Ranta et al., 1995), fish (Ranta et al., 1995), mammals (Haydon et al., 2001; Grenfall et al., 1998) and insects (Benton et al., 2001). Ecologists have applied synchronisation theory to a variety of terrestrial ecosystems by modelling an area of interest as a spatially-extended metapopulation of discrete populations, interacting directly or indirectly via, for example, migration or a common environmental forcing. Clearly, this is directly analogous to how plankton ecosystems are typically modelled. Given this, what can synchronisation theory tell us about the emergent spatial structure seen in these simulations and in the ocean?

Initial studies addressing this question have focused on spatial synchrony for the simple case of a one-dimensional chain of identical plankton populations coupled by a nearest neighbour flux (Hillary and Bees, 2004a,b; Guirey et al., 2007). Hillary and Bees (2004a) calculated the stability of fully synchronised dynamics for a chain of identical chaotic populations as a function of the strength of interaction between them. It was found that a critical coupling strength was required for stably homogeneous dynamics. Their results suggested some dependence of this critical coupling on the number of populations. A study by Guirey et al. (2007) confirmed this, showing that the required coupling increased with the number of populations. Guirey et al. (2007) also showed that the choice of grid-cell biological representation and parameters has a strong influence on the spatial dynamics of the simulation. A worrying consequence for modelling studies is that a simulation could exhibit patchy or stably homogeneous dynamics depending on possibly arbitrary choices of the spatial resolution and biological model parameters.

Here, we apply the methods of synchronisation theory to a plankton distribution modelled as a two-dimensional lattice of interacting oscillatory populations. This is immediately more oceanographically relevant and applicable to typical biophysical plankton studies. This study deals in particular with coupled *regularly oscillating* populations. Oscillatory dynamics occur generically in plankton population models (e.g. Ryabchenko et al., 1997; Totterdell, 1993; Steele and Henderson, 1992) so it is important to understand their coupled behaviour, and empirical work provides evidence for oscillatory dynamics in real-world populations (e.g. Fussman et al., 2000; Ylikarjula et al., 2000). We also introduce spatial variation in dynamics by allowing the biological parameters to vary across the lattice. Previous work (Hillary and Bees, 2004a; Guirey et al., 2007) has represented the populations as identical oscillators; this implies that the same set of parameter values represents the biological dynamics equally well across the whole modelled region. In reality, spatial variation is inherent in nature so that the most appropriate set of biological parameters is likely to vary in space. Initial work (Hillary and Bees, 2004b) applied parameter mismatch to the zooplankton mortality rate in a chain of plankton populations. For certain values of coupling, phase synchronisation was found to occur, with populations frequency-locked and in-phase but with different amplitudes. This is a phenomenon commonly observed in terrestrial ecological data (Elton and Nicholson, 1942). Here, we apply mismatch to the phytoplankton growth rate of each population in order to represent simply the kind of small-scale biological variability that may arise from physical variability, for example in mixed layer depth. This mismatch leads to a spread in the amplitude and period of oscillation of the uncoupled populations. A two-dimensional coupled system of non-identical oscillators was first studied in a terrestrial context by Blasius et al. (1999), looking in particular at the effect of the rate of migration between populations on the spatio-temporal dynamics of the simulation. Frequency-locking and full synchronisation were found to occur, depending on the rate of migration, with frequency-locking leading to large quasi-regular travelling waves of synchronised dynamics.

We would like to understand how the parameters of the stripped-down biophysical plankton model influence the emergent spatial structure and in particular the occurrence of plankton patchiness. This study focuses on the strength of interaction, representing the effects of the physical flow, between populations and the associated length-scale of the grid-cell. The emergent spatial dynamics of the simulation, characterised in terms of the dominant length-scale of spatial structure and the altered amplitudes and periods of oscillation of the coupled populations, is investigated as a function of the rate of interaction between populations. We show that interaction between these non-identical populations can result in persistent clustering of populations into pockets of locally synchronised dynamics. The occurrence and length-scale of this patchiness is found to vary unpredictably with changes in the strength of interaction, a result which is of interest and concern to biophysical modellers hoping to reproduce plankton patchiness and its consequences in their models.

2. Methods

Following the standard approach to plankton ecosystem modelling, we simulate a spatially varying surface ocean distribution of plankton as a lattice of interacting plankton sub-populations. The biological dynamics of each sub-population is represented by the same Nutrient–Phytoplankton–Zooplankton (NPZ) model (see Eqs. (1)–(3)), originally formulated by Steele and Henderson (1981).

$$\begin{aligned}\frac{dN}{dt} &= -\frac{a_0 N}{(e+N)(b+cP)}P + rP + \frac{\zeta\beta P^2}{\mu^2+P^2}Z + \gamma dZ + k(N_0 - N)\\ &= -\text{uptake} + \text{respiration} + Z \text{ excretion}\\ &\quad + Z \text{ predators excretion} + \text{mixing},\end{aligned} \tag{1}$$

$$\begin{aligned}\frac{dP}{dt} &= \frac{a_0 N}{(e+N)(b+cP)}P - rP - \frac{\zeta P^2}{\mu^2+P^2}Z - sP - kP\\ &= \text{uptake} - \text{respiration} - \text{grazing by } Z - \text{sinking} - \text{mixing},\end{aligned} \tag{2}$$

$$\begin{aligned}\frac{dZ}{dt} &= \frac{\zeta\alpha P^2}{\mu^2+P^2}Z - dZ\\ &= \text{growth due to grazing on } P - \text{higher predation}.\end{aligned} \tag{3}$$

Briefly, this is a zero-dimensional model representing, by a system of ordinary differential equations, the processes occurring in a physically homogeneous region of upper ocean mixed layer. An implicit biologically inactive deeper layer with a fixed nutrient content acts by way of vertical mixing as a nutrient source for the upper layer biology. The change in phytoplankton concentration is modelled as the sum of growth, co-limited by nutrients and light (represented

as a self-shading term), and losses due to respiration, mixing and sinking out of the upper layer, and grazing by zooplankton. Of the material grazed by zooplankton, a fixed fraction is assimilated, contributing to zooplankton growth. A parameterisation of predation by higher predators closes the food chain from above. A fixed proportion of the material grazed by zooplankton and higher predators is excreted back to the nutrient pool. The zooplankton are assumed to possess enough mobility to remain within the mixed layer.

A fuller description of the NPZ model can be found in Steele and Henderson (1981) and subsequent explorations by Edwards and Brindley (1996) and Edwards (2001). See also Guirey et al. (2007) for a study of synchronisation of identical plankton populations using this and alternative plankton models for a range of biological model parameters. For the purposes of the work presented here we use a default parameter set (Table 1) for which the model exhibits regular oscillatory behaviour. This is the simplest time-varying behaviour possible that is not due to any external forcing. We stress that this study is intended to be illustrative; we do not attempt to accurately model the seasonal cycle of plankton dynamics in the surface ocean.

The general set-up is a region of surface ocean of size L km $\times$ L km modelled as a two-dimensional lattice of $n \times n$ non-identical interacting populations, giving spatial resolution $\frac{L}{n}$. To incorporate the spatial variation inherent in nature, we allow the biological model parameters to vary across the modelled domain: a small mismatch is added to the default phytoplankton growth rate a_0 for each population. This is justified on the basis that phytoplankton growth has been shown to vary with such factors as temperature (Eppley, 1972) and mixed layer depth (Alpine and Cloern, 1988), which vary on the submeso- and mesoscale. Making no assumptions about the source of the spatial variation, the phytoplankton growth rates $a_{i,j}$ are chosen at random from a uniform distribution of width Δ centred on a_0 so that $a_{i,j} \in [a_0 - \frac{\Delta}{2}, a_0 + \frac{\Delta}{2}]$ for $i,j = 1\ldots,n$.

Components of this framework are typical of any marine biophysical simulation: number of grid-cells, strength of interaction between these grid-cells, spatial resolution, representation of physical flow and biological dynamics. Here we focus in detail on the impact of varying the strength of interaction between grid-cells and the associated spatial resolution. We set $n = 100$, a number of grid-cells chosen so that the ensemble remains small enough to be computationally inexpensive but large enough to give an unbiased sample of the probability distribution underlying $a_{i,j}$. The central phytoplankton growth parameter is $a_0 = 0.2$. The spread Δ in growth rate values is chosen as 5% of a_0, giving $a_{i,j} \in [0.195, 0.205]$. The choice of Δ is deliberately conservative so that each sub-population essentially has the same type of dynamics but with a small difference in amplitude and period of oscillation. For this range, the biological model has oscillatory dynamics. The spread in natural (uncoupled) frequencies is $\approx$2.5% with mean angular frequency $\omega = 0.052$ 2π d^{-1}. In the absence of interaction between populations, even for this small spread in natural properties, a simulation run from initially homogeneous conditions leads quickly to a random field of abundances.

The populations interact via a nearest neighbour coupling term, with no-flux boundary conditions on all edges of the domain (identical results are obtained for periodic boundary conditions):

$$\dot{v}_{i,j} = F_{i,j}(v_{i,j}) + \varepsilon \cdot (v_{i-1,j} + v_{i+1,j} - 4v_{i,j} + v_{i,j-1} + v_{i,j+1}),$$

where $v_{i,j} = (N_{i,j}, P_{i,j}, Z_{i,j})$, the function $F_{i,j}$ is the NPZ model described above with phytoplankton growth rate $a_{i,j}$ and ε is the strength of interaction between populations. The coupling term represents mixing processes between adjacent grid-cells so that

$$\varepsilon \cdot (v_{i-1,j} + v_{i+1,j} - 4v_{i,j} + v_{i,j-1} + v_{i,j+1}) \approx D\frac{\partial^2 v_{i,j}}{\partial x^2},$$

where D is the effective diffusivity between grid-cells. Hence we may equate ε with the effective diffusivity so that

$$\varepsilon \approx \frac{D}{l^2},$$

where $l = \frac{L}{n}$ is the grid-cell length-scale and $\frac{1}{l^2}$ approximates the second order spatial derivative. The effective diffusivity has been shown by Okubo (1971) to scale with spatial length-scale according to the empirical relationship

$$D(l_s) \approx 0.01 l_s^{1.15},$$

with l_s in cm and effective diffusivity $D(l_s)$ in cm^2 s^{-1}. If we then take the grid-cell length-scale l km of the lattice as the spatial scale at which effective diffusivity acts in the model, then

$$\varepsilon \approx 0.01 l^{-0.85} \times 60 \times 60 \times 24,$$

for ε in d^{-1}. For mesoscale processes on the order of 1–100 km, this gives a range of coupling $\varepsilon \in [0.001, 0.05]$ d^{-1} between adjacent grid-cells with coupling strength increasing with decreasing length-scale. Varying ε in this range is equivalent to varying the spatial resolution of the model from 100 to 1 km, i.e. $l \in [1, 100]$ km. However, since an understanding of the uncoupled system ($\varepsilon = 0$) is essential to an understanding of the coupled system ($\varepsilon > 0$), we consider the range $\varepsilon \in 0 \cup [0.001, 0.05]$ d^{-1}.

For each value of ε, the system is integrated from an initially spatially homogeneous state until transient dynamics die away. Results were found to be insensitive to choice of initial conditions. The resultant behaviour of the simulation for these different strengths of interaction between populations is characterised using several diagnostics, which are described here and summarised in Table 2. See the Appendix for full definitions.

A visual indication of spatial structure is obtained from the two-dimensional fields of phytoplankton, nutrient and zooplankton concentrations in time and space.

Frequency-locking is checked for by calculating frequency of oscillation $\Omega_{i,j}$ of each sub-population and the relative standard

Table 1
Biological model parameters.

Parameter	Symbol	Value	Units
P growth parameter	a_0	0.2	m^{-1} d^{-1}
Light attenuation by water	b	0.2	m^{-1}
Self-shading by P	c	0.4	m^2 gC^{-1}
Herbivorous Z mortality	d	0.14	d^{-1}
N half-saturation constant	e	0.03	gC m^{-3}
Exchange rate with lower layer	k	0.05	d^{-1}
P respiration	r	0.15	d^{-1}
P sinking	s	0.04	d^{-1}
Lower layer N concentration	N_0	1.0	gC m^{-3}
Herbivorous Z assimilation efficiency	α	0.25	–
Z excretion fraction	β	0.33	–
Remineralisation of Z excretion	γ	0.5	–
Herbivorous Z grazing rate	ζ	0.6	d^{-1}
Herbivorous Z grazing half-saturation constant	μ	0.035	gC m^{-3}

Table 2
Summary of diagnostic statistics.

Measure	Symbol	Range	Units
Phytoplankton biomass of population (i,j)	$P_{i,j}$	0–0.5	gC m^{-3}
Angular frequency of population (i,j)	$\omega_{i,j}$	0.05–0.15	2π d^{-1}
Frequency spread	σ	0–25	%
Phase order	R	0–1	–
Cluster measures	c_x, c_y	1–n	Grid-cells
Gradient measure	g	0–1	–

deviation σ of these frequencies. The populations are *frequency-locked* when $\sigma = 0$.

The phase of oscillation of each population is determined and used to calculate a measure R of the phase coherence of the ensemble (Pikovsky et al., 2001). See Appendix for a fuller definition. $R = 1$ for a *phase-locked* ensemble. For uncorrelated populations, the phases are uniformly distributed on $[0, 2\pi]$ so R is close to 0. Intermediate values of R indicate some degree of local synchrony or clustering of phases.

Whilst σ and R give an indication of the coherency of behaviour of the ensemble as a whole, they can mask *local* synchronous effects such as clustering of the domain into synchronised subsets of populations. This is precisely the spatial variability in which researchers into plankton patchiness are interested. Hence, we use two simple measures, c and g, of spatial structure. The cluster measure $c \in [1, 100]$ of grid-cells measures the mean size of clusters or patches in one-dimension. It may be calculated in either dimension of the lattice to give c_x and c_y. For zero coupling, $c = 1$ grid-cell because populations oscillate independently and so there is no spatial structure larger than the scale of underlying variability. If the whole ensemble is synchronised (spatially homogeneous), we expect a c value of the length of the domain, i.e. $c = 100$. $c \in (1, 100)$ indicates some level of local synchronisation (patchiness). The gradient measure $g \in [0, 1]$ measures the sharpness of transition in state variable values between patches (see Appendix for more details).

Used together, these tools allow us to describe in detail the emergent spatial structure of the simulation as the strength of interaction between the plankton populations is varied.

3. Results

3.1. Temporal evolution of spatial structure

Fig. 1 gives an example of how spatial structure emerges from the initially homogeneous state; the phytoplankton field is shown at 100 day intervals for an example coupling strength of $\varepsilon = 0.01\ \mathrm{d}^{-1}$. Similar spatial properties are observed for the nutrient, phytoplankton and zooplankton biomass values, so results are presented only for phytoplankton for brevity. The initial domain-sized structure breaks down into clusters. Circular regions appear, containing small-scale clusters, which are themselves not circular but appear as elongated shapes. These circular regions grow, increase in number and merge until the domain is filled with the small-scale clusters, which appear to reach a constant size at around $t = 2,000$ days. See Section 4 for a discussion of the long time-scale of these transient dynamics. The calculated cluster measures $c_x(t)$ and $c_y(t)$ plotted in Fig. 2 confirm what can be seen visually: the structure in both directions reaches an equilibrium length-scale of 4–5 grid-cells. Relating the coupling strength $\varepsilon = 0.01$ to a grid-cell length-scale of around 6.4 km using the Okubo relationship, this gives a steady-state cluster size of ≈25–32 km. The clusters are synchronised regions, with sharp transitions at their boundaries, as indicated by a value of $g(t) \approx 0.85$ in Fig. 2. Although the cluster size converges, the position of these clusters is non-stationary, indicating that the spatial arrangement of the structure is not a simple reflection of the spatial arrangement of the underlying natural frequencies; larger scale patchiness has emerged from the interaction of small-scale variability and dispersal between populations, and the clustering structure continues to evolve in time after the spatial structure mean size has reached a steady-state. In other words, the patches appear, move and disappear, but the characteristic spatial length-scale remains constant. The time-evolution plots clearly show that $\varepsilon = 0.01\ \mathrm{d}^{-1}$ is not a strong enough coupling to counteract the natural frequency disorder and keep the system in full synchronisation despite the small spread in natural frequencies.

3.2. Equilibrium spatial structure as a function of coupling strength

Fig. 3 shows how the frequency spread σ, phase order parameter R, the frequencies of the oscillators and the spatial measures c_x, c_y and g, for the system having reached steady-state, vary as a function of coupling strength for $\varepsilon \in [0, 0.05]\ \mathrm{d}^{-1}$. Calculation of the measures is made once the system has been judged to reach a statistical steady-state, e.g. after 2000 days for the example of $\varepsilon = 0.01\ \mathrm{d}^{-1}$ given above. The transient length was found to vary with ε so that, especially near to bifurcations in system behaviour (see below), an integration of up to 5000 days was required for the measures to approach equilibrium.

It is immediately seen that increasing the coupling strength does not have the intuitive effect of monotonically increasing the degree of synchrony exhibited by the ensemble: we do not have a monotonic decrease in σ and increase in R as ε is increased. Over the range of ε, the diagnostic tools and spatial phytoplankton biomass plots indicate that the dynamics of the ensemble exhibits several qualitatively different states. The equilibrium phytoplankton field for values for $\varepsilon = 0\ \mathrm{d}^{-1}$, $\varepsilon = 0.001\ \mathrm{d}^{-1}$, $\varepsilon = 0.002\ \mathrm{d}^{-1}$, $\varepsilon = 0.01\ \mathrm{d}^{-1}$ and $\varepsilon = 0.04\ \mathrm{d}^{-1}$, for which the system enters each of the states described below, respectively, are shown in Fig. 4.

- $\varepsilon = 0\ \mathrm{d}^{-1}$: independent populations.
  For zero coupling the plankton populations oscillate independently, so that the phytoplankton field shown in Fig. 4a is random with no spatial structure larger than the grid-cell, as confirmed by c_x and c_y values of 1 in Fig. 3. As expected, $\sigma \approx 2.5\%$. Since there is no interaction between neighbouring populations, there can be a sharp transition in phytoplankton biomass from grid-cell to grid-cell, indicated by gradient measure value of $g = 1$ (Fig. 3).
- $0.001 \leqslant \varepsilon < 0.002\ \mathrm{d}^{-1}$: small increase in frequency spread; small-scale clustering.
  For $0.001 \leqslant \varepsilon < 0.002$ the spread in frequencies increases with increased coupling strength (Fig. 3). The frequencies are seen in general to increase and the frequency spread, σ, increases to more than 5%. Despite the increase in σ, the clustering in the biomass plots indicates that the size of spatial structure in the phytoplankton field has increased (Figs. 3 and 4b). The increase in coupling has caused an increase in local synchronisation although the size of the clusters remain small at 2–3 grid-cells. These clusters are well-defined, as indicated by $g = 1$ in this region (Fig. 3).
- $0.002 \leqslant \varepsilon \leqslant 0.0025\ \mathrm{d}^{-1}$: frequency-locking; medium-scale clustering.
  For coupling around $\varepsilon = 0.002\ \mathrm{d}^{-1}$ there is a small region of near frequency-locking, seen by a rapid decrease in σ to $< 1\%$ (Fig. 3). The scale of spatial structure increases; the phytoplankton biomass field shows much larger clusters (Fig. 4c) and the cluster measure increases to $c_x = c_y = 10$ grid-cells (Fig. 3). However, the system is clearly not phase-locked since neighbouring clusters coexist with some at their peak in phytoplankton biomass and some at their trough, confirmed by an order parameter value of $R \approx 0.6$ (Fig. 3), with sharp transitions at cluster boundaries indicated by $g = 0.9$ (Fig. 3). The spatio-temporal pattern here is of numerous interfering "target patterns" or travelling waves. The clusters are characteristically quasi-regular, unlike the irregularly-shaped clusters seen for $0.001 \leqslant \varepsilon < 0.002\ \mathrm{d}^{-1}$ and $0.0025 < \varepsilon < 0.02\ \mathrm{d}^{-1}$.
- $0.0025 < \varepsilon < 0.02\ \mathrm{d}^{-1}$: large frequency spread; small-scale clustering.
  Note that the dynamics shown in Fig. 1 occupies this small-scale clustering region.

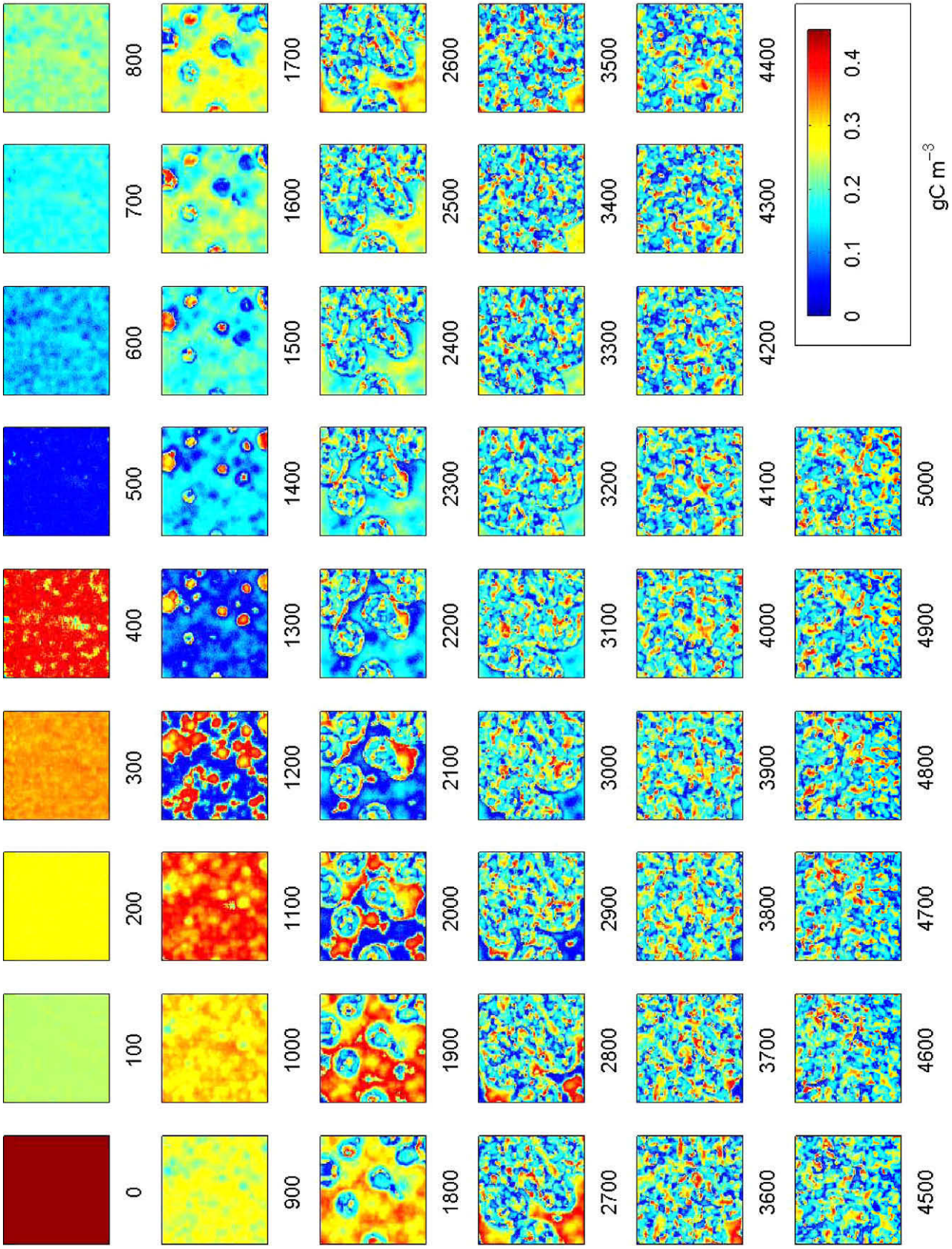

Fig. 1. Temporal dynamics. Evolution of phytoplankton biomass field for 5000 days from initially homogeneous conditions for a lattice of 100 × 100 populations interacting with effective diffusivity $\varepsilon = 0.01\ \mathrm{d}^{-1}$. Figure labels indicate time in days.

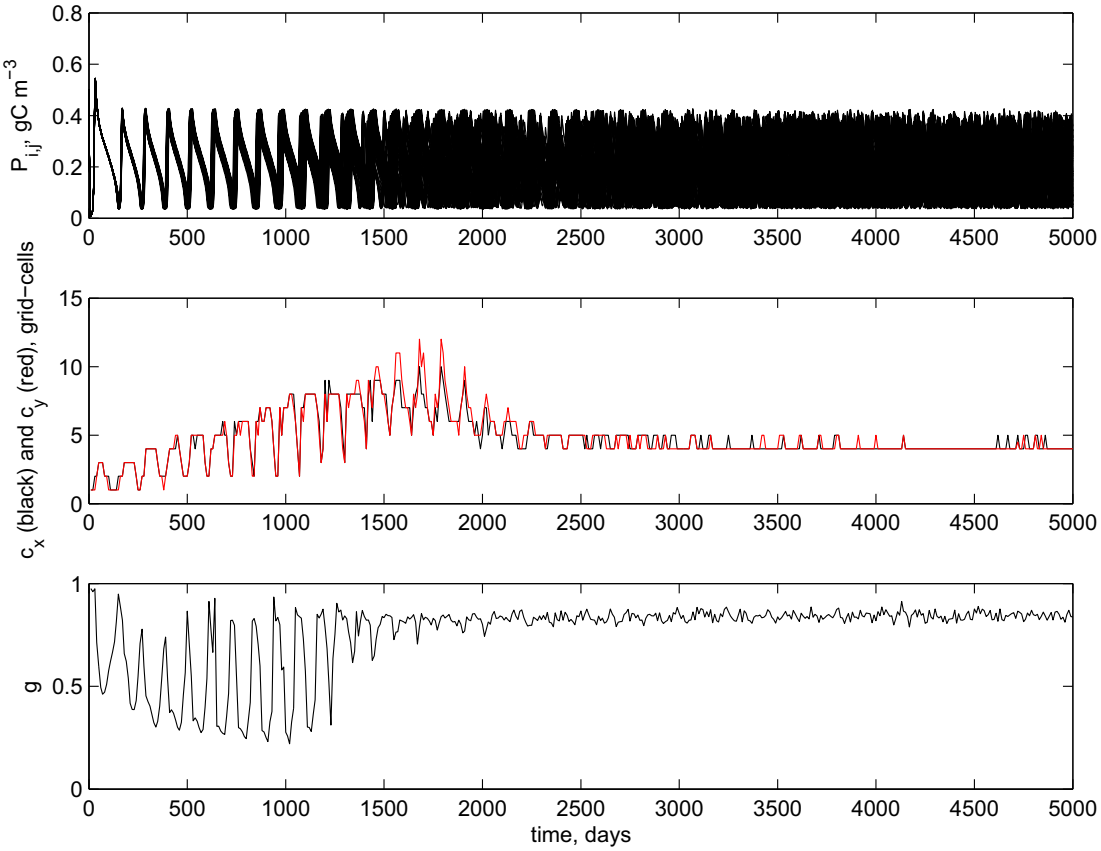

Fig. 2. Temporal dynamics. Evolution of spatial structure for 5000 days from initially homogeneous conditions for a lattice of 100×100 populations interacting with effective diffusivity $\varepsilon = 0.01\ \mathrm{d}^{-1}$, showing phytoplankton biomass $P_{i,j}(t)$ for $i,j = 1,\ldots,100$, cluster measures $c_x(t)$ and $c_y(t)$ and gradient measure $g(t)$).

As ε is increased above $0.0025\ \mathrm{d}^{-1}$, the ensemble bursts out of frequency-locking and enters a desynchronised region for $\varepsilon \in (0.0025, 0.02)\ \mathrm{d}^{-1}$. The spread in frequencies reaches an order of magnitude higher than the spread in independent frequencies and increasing ε within this region apparently has no effect on the amount of disorder in the frequencies (Fig. 3). However, clustering is clearly visible in the phytoplankton distribution snap-shots for coupling in this region (e.g. $\varepsilon = 0.01$; Fig. 4d). Additionally, although σ gives no evidence of an increase in the amount of synchrony for increased coupling, the phytoplankton fields clearly show an increase in the size of clusters as ε is increased; the amount of local synchrony in both the x and y directions increases and c_x and c_y increase slowly and monotonically from 2 to 7 grid-cells (see Fig. 3). However, the actual cluster size monotonically *decreases* from around 50 to 20 km because the grid-cell length-scale decreases with increasing ε. The gradient measure remains high ($g > 0.7$) in this region as clusters are still well-defined (Fig. 3).

- $0.02 \leqslant \varepsilon \leqslant 0.05\ \mathrm{d}^{-1}$: frequency-locking; near domain-sized spatial dynamics; near phase-locking.

  At $\varepsilon = 0.02$ there is a rapid, threshold-like transition to a frequency-locked state, with a decrease in σ to near zero. The dynamics are largely synchronised, with no sharp transitions between neighbouring grid-cells, unlike in the clustering state (e.g. $\varepsilon = 0.04$; Fig. 4e). We see a rapid decrease in g at this threshold to values around 0.3 (Fig. 3), showing that changes in phytoplankton biomass occur more smoothly across the lattice. c_x and c_y increase rapidly to approximately half the domain size at this threshold (Fig. 3), indicating a rapid increase in dominant spatial structure. The system remains frequency-locked for increased coupling after this transition and the resultant frequency of the synchronised system tends towards the mean of the natural frequencies, $\Omega = 0.052$.

  In contrast to the threshold-like change to frequency-locking, the transition to phase-locking after $\varepsilon = 0.02$ is gradual, as seen by a slow monotonic increase in R towards 1 (Fig. 3). For coupling in the range considered here of $\varepsilon < 0.05$, we see that the ensemble never achieves fully phase-locked dynamics, as $R < 1$ (Fig. 3) and the variation in colour in the biomass plots for ε in this region always indicates some variation in the phase of oscillation of the populations across the domain.

  The spatio-temporal dynamics for this range of coupling are as described for $0.002 \leqslant \varepsilon \leqslant 0.0025$ above: travelling quasi-regular waves of synchronised abundances. However, the length-scale of the waves is much larger for this range of stronger coupling.

4. Discussion and conclusions

Using a standard approach to plankton ecosystem modelling, a distribution of plankton has been modelled as a lattice of interacting non-identical oscillatory populations, each represented by the same NPZ model but with a spread of phytoplankton maximum growth rates. Typical characteristics of a biophysical simulation such as spatial resolution, grid-cell biological model and representation of the physical flow are often selected for subjective or non-oceanographic reasons like available computing power or common usage in the literature. It is important that biophysical modellers examine and understand the sensitivity of modelling results to these model components. The aim of the study has therefore been to explore how the emergence of spatial structure in biophysical simulations is a function of the underly-

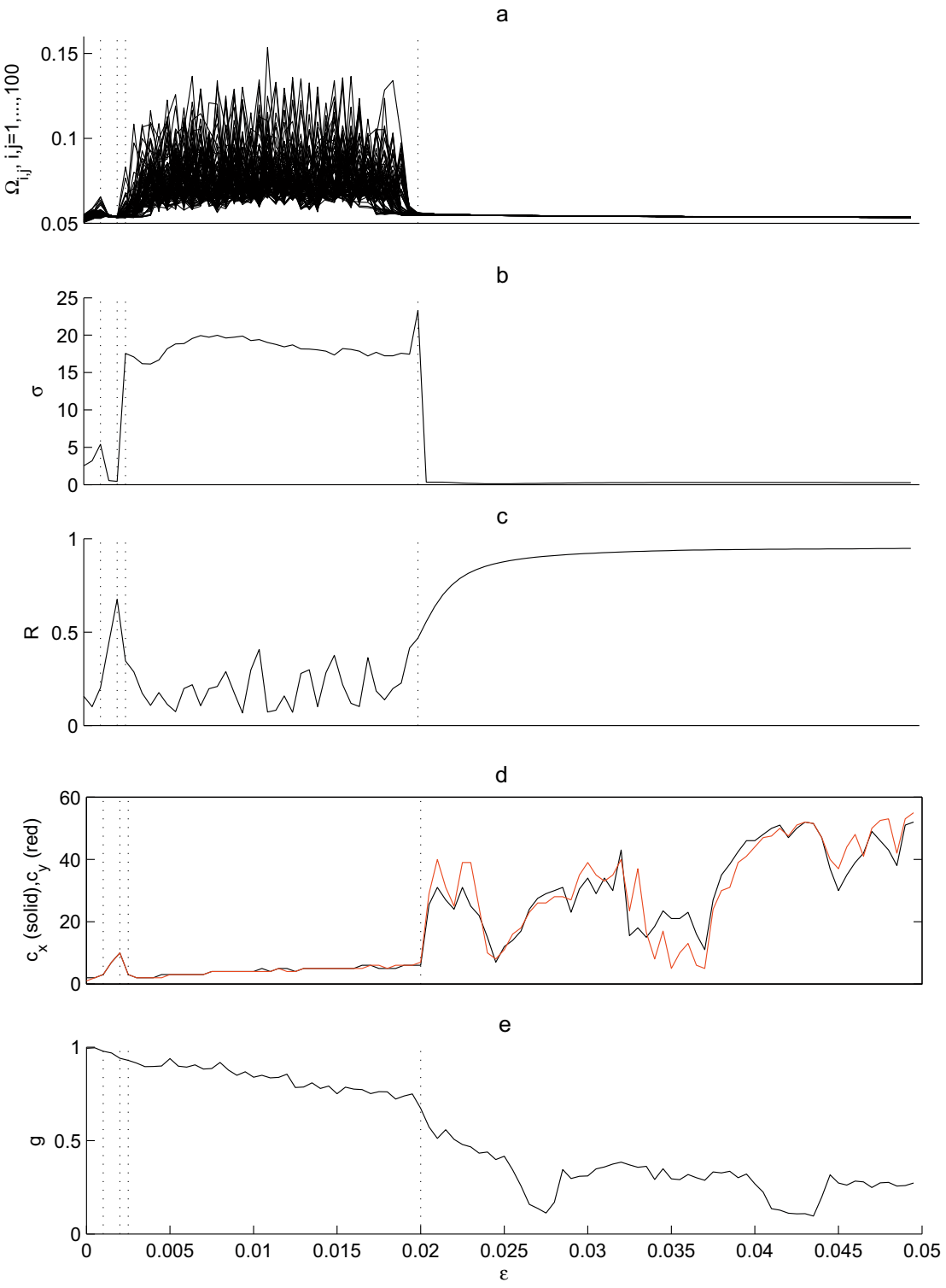

Fig. 3. Diagnostics for $n = 100$ as a function of coupling strength. Frequencies ω_{ij} for $i, j = 1, \ldots, 100$, frequency spread σ, order parameter R, cluster measures $c_x(\varepsilon)$ and $c_y(\varepsilon)$ and gradient measure $g(\varepsilon)$ for $\varepsilon \in [0, 0.05]$ d^{-1}. Dotted lines mark the transitions between the different types of equilibrium dynamics described in Section 3.

ing model structure. The results have shown an unusual but potentially problematic mechanism for the formation of plankton patchiness.

In this study, we have focused on the impact of the rate of dispersal between populations and the associated spatial scale of the grid-cell. The numerical experiment has shown that altering the strength of interaction between populations alters the emergent spatial structure of the simulation. An increase in the strength of interaction does not lead to a monotonic increase in synchrony: remarkably, interaction between populations has been shown for some coupling strengths to increase the frequency disorder of the ensemble by an order of magnitude in comparison with the natural (uncoupled) level. Eventually, as the coupling strength is increased beyond a critical value, intuitive behaviour returns and

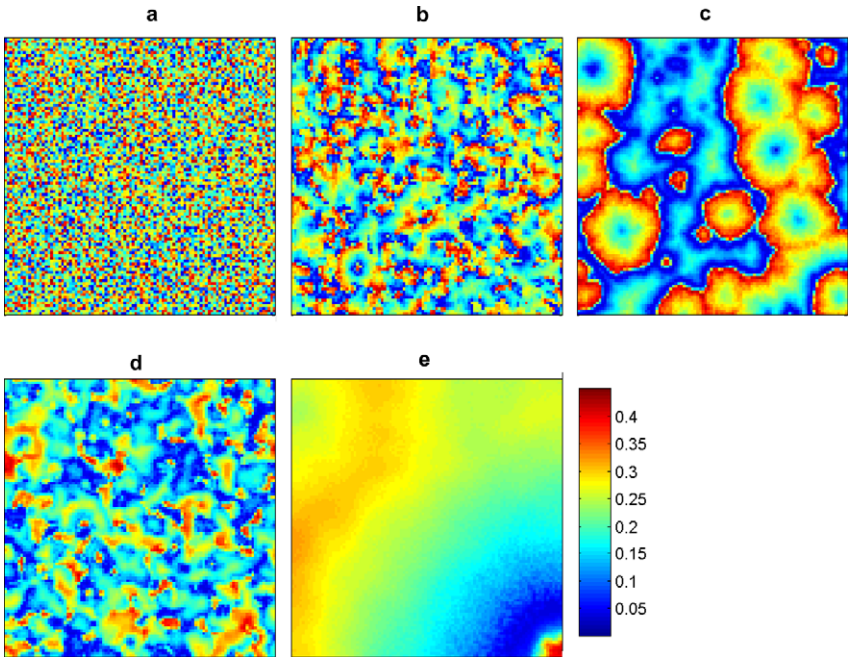

Fig. 4. Phytoplankton biomass field (gC m^{-3}) for effective diffusivity (a) $\varepsilon = 0\ d^{-1}$, (b) $\varepsilon = 0.001\ d^{-1}$, (c) $\varepsilon = 0.002\ d^{-1}$, (d) $\varepsilon = 0.01\ d^{-1}$ and (e) $\varepsilon = 0.04\ d^{-1}$.

the system locks into frequency synchronisation. Since the coupling strength is inversely related to the grid-cell length-scale, the existence of a critical coupling strength implies the existence of a critical spatial resolution for frequency-locking: for high enough spatial resolution, the frequency disorder does not occur.

The non-monotonic response of the system to coupling strength has been observed for a system of non-identical foodweb oscillators by Blasius and Montbrió (2003) and termed an "anomalous transition to synchronisation": increased coupling was seen to first increase the amount of frequency disorder before larger coupling was able to draw the system into synchrony. In that study, however, only the *system-level* behaviour was explored, with no examination of the *local* effects or the spatial structure. Here, we have seen that the anomalous region of apparent desynchronisation manifests as clustering of nearby populations into persistent pockets of synchronised dynamics. The interplay between the built-in spatial variation (the spread in phytoplankton growth rates) and the dispersal between populations results in patchiness which is temporally evolving but has a stable characteristic length-scale. The spatial structure of the patchiness is emergent and is not directly generated by any underlying structure in the parameters of the uncoupled populations. Although in a real-world distribution these parameters may be expected to be spatially correlated, for this study they were deliberately chosen from a random distribution to avoid introducing another spatial scale into the system. This is the simplest and clearest case for an initial study and ensures that any spatial structure in the simulations is emergent and not a direct corollary of any imposed spatial structure.

When the system is frequency-locked, the spatio-temporal dynamics consist of quasi-regular travelling waves of phase synchronisation. These waves appear on different spatial scales depending on the strength of coupling. Blasius et al. (1999) and Blasius and Tönjes (2005) observed this type of dynamics in a two-dimensional simulation of coupled non-identical predator–prey populations and identified the structure as being caused by entrainment of surrounding populations by fast-paced "pace-maker" oscillators. In the simulations presented here, it appears that for small coupling ($\epsilon \approx 0.002\ d^{-1}$), many oscillators act as such pace-makers, resulting in a pattern of interfering travelling waves. For larger coupling ($\epsilon \approx 0.002\ d^{-1}$), one dominant pace-maker controls the other populations, resulting in a travelling wave with a single epi-centre. As Blasius and Tönjes (2005) point out, it is unintuitive that quasi-regular behaviour should emerge in a coupled system of oscillators with no imposed directionality or spatial correlation in frequency distribution. It is equally unintuitive that the previously-unobserved *irregular* clustering should occur for a coupling range ($0.0025 < \varepsilon < 0.02$) between two regimes of regular travelling waves.

Importantly, although there is a gradual increase in the cluster size within the anomalous region of coupling as the coupling strength is increased, the transition to large-scale structure is not continuous but occurs abruptly at the threshold coupling strength. In consequence, the emergent features of a biophysical simulation can alter discontinuously as the coupling strength is varied. Since the coupling strength is related to spatial scale, altering the spatial resolution of a simulation could therefore have unpredictable consequences for the model results and, importantly, for conclusions and predictions drawn from them. For example, the presence of such discontinuities is of concern if a model is to be used to study length-scales of plankton patchiness since increasing the model resolution could obliterate the patches, even if the patch length-scale is significantly larger than the grid-cell. More generally, it is worrying that the subjective choice of spatial resolution affects the scale of patchiness.

The clustering behaviour has also been found to occur for different modelling scenarios (Guirey, 2007): for a fixed area of ocean with varying number of grid-cells and therefore spatial resolution, for a large number of differently seeded random mismatch values, and for parameter mismatch applied to a different biological model parameter. This suggests that this mechanism for patchiness potentially occurs generically in biophysical ocean simulations. However, these experiments showed that the critical value for the transition to frequency-locking, i.e. the threshold between patchiness and domain-scale structure, is very sensitive to the model.

This study deals directly only with oscillatory plankton populations. This makes it widely applicable; regular oscillatory dynamics occur generically in plankton population models and have been

seen to occur in the real-world (see Section 1). To check further applicability of the results of the simulations, alternative coupled dynamics need to be explored. However, evidence suggests that the results are more generally applicable. For example, spatial synchronisation effects, in general, have been observed for coupled chaotic plankton populations (e.g. Hillary and Bees, 2004a; Guirey et al., 2007). As part of the present study, the clustering behaviour, in particular, was also found to occur with a set of biological model parameters giving chaotic rather than cyclic population dynamics. Additionally, synchronisation effects in population dynamics have been shown to persist for other types of time-varying behaviour including driving by stochastic noise or deterministic forcing (Blasius et al., 1999; Hillary and Bees, 2004a).

For the simulations presented here, the equilibrium dynamics of the system take a long time (≈2000 days) to become established. This is partly due to the long (≈120 day) period of oscillation of each sub-population and it is hypothesised, although not explored here, that a shorter period of oscillation would lead to a shorter transient time. Long transients are expected in systems of non-identical oscillators with similar frequencies: the difference in frequency between oscillators is typically of order $\Delta\Omega = 10^{-3}$, which, following Blasius and Tönjes (2005), gives the transition time to equilibrium $T \sim (\Delta\Omega)^{-1}$ of the order of 100 days. The length of the transient varies with the coupling strength; close to the threshold-like bifurcations in system behaviour, the statistical steady-state takes longer to become established. These long time-scales might lead us to question the relevance of the equilibrium spatial structure to real-world plankton populations with a seasonal period of 365 days. However, it is clear from Fig. 1 that much of the spatial structure at the eventual steady-state length-scale emerges on much shorter time-scales of order 100 days. It must also be stressed that the results of this study should be taken as illustrative of the kind of synchronous effects that occur in biophysical modelling; the system studied here is not intended to reproduce the seasonal dynamics of surface ocean plankton and the period of oscillation of a sub-population has not been tuned to any particular time-scale. The application of external (seasonal) forcing to this system should be a focus of future work. Such a system-level forcing acts as an additional, indirect, form of coupling between sub-populations (the Moran effect; Moran (1953)), so it is very likely that synchronous effects similar to those seen in this study will occur.

From this study, we may draw two conclusions.

Firstly, synchronisation effects may be a genuine mechanism for plankton patchiness and explain some of the spatial structure seen in real-world plankton distributions. To confirm this, future work should look at increasing the realism of the representation of the flow. Given the range of complex phenomena possible in fully turbulent models, this is beyond the scope of this paper. However, initial investigations (manuscript in preparation and see Guirey, 2007) into the impact of a simple advective flow at scales larger than the grid-cell suggest that stable clustering is able to persist under this influence. Future work should also look at the impact of large-scale seasonal forcing on the emergence of clustering. An alternative approach would be a synergistic satellite data study: altimeter-derived or modelled horizontal current velocities could be used to characterise a region of ocean in terms of the strength of coupling between populations at different points in space and time. With a suitable representation of the biological dynamics of the region, making comparisons with satellite ocean colour chlorophyll data, such a set-up could be used to further explore how emergent structure in real plankton distributions may be understood in terms of synchronisation phenomena. The results presented here would form a firm basis for such work.

Secondly, we have clearly shown that the emergent spatial structure is very sensitive to the underlying model structure, with abrupt and somewhat unpredictable changes from patchy to homogeneous dynamics as key parameters of the simulation are varied. This was also seen in previous studies of the simpler one-dimensional case (Hillary and Bees, 2004a,b; Guirey et al., 2007). It is therefore clearly difficult for models to reproduce plankton patchiness objectively. Modellers should therefore be aware of the possibility of artificial patchiness arising from the basic physical structure of their model. Although spatial structure in plankton concentration related to hydrographic features such as eddies and fronts may be "real", structure unrelated to such obvious features may be spurious. For example, spurious small-scale structure may cause errors in studies aiming to reproduce spatial spectra for plankton in the ocean (e.g. Martin and Srokosz, 2002; Tzella and Haynes, 2007). At this stage, it is difficult to say what spatial resolution should be used to "best" model plankton patchiness; it would be unwise to artificially eliminate or encourage particular spatial properties until they have been more closely tied to real-world plankton dynamics. Without future work investigating the influence of large-scale seasonal forcing and explicit advection, it is also impossible at this stage to give clear advice about the conditions under which clustering may arise in a biophysical simulation.

Overall, our results indicate that whilst cluster synchronisation may be a genuine mechanism for the formation of plankton patchiness and thus of relevance to real-world observations, modellers need to be aware that artificial patchiness could also arise in simulations through the same mechanism. More generally, this study reaffirms the importance of sensitivity analysis in biophysical modelling.

Acknowledgements

The author E.J.G. is grateful for an Environmental Mathematics and Statistics (EMS) Programme Studentship jointly funded by NERC and EPSRC. This manuscript forms part of the contribution by the National Oceanography Centre, Southampton, (MAS and APM) to Theme 2 of the Oceans 2025 programme funded by NERC. The author M.A.B. acknowledges EPSRC funding EP/D073398/1. We thank Andreas Oschlies and two anonymous reviewers for constructive comments that greatly improved the manuscript.

Appendix A. Diagnostics for synchrony

The average angular frequency $\omega_{i,j}$, $i,j = 1,\ldots,n$, of each oscillator in the $n \times n$ lattice is calculated in order to check for frequency-locking of the ensemble. During integration of the system, a note is made of times when each oscillator reaches a peak in its phytoplankton concentration. This gives a series $\{T_{i,j}\}$ of peak times for each oscillator which is used to calculate the average frequency

$$\omega_{i,j} = \left(\frac{N-1}{T_{i,j}(N) - T_{i,j}(1)}\right) \times 2\pi,$$

where there are N peaks in the series.

The average rather than instantaneous frequency is calculated in case any of the oscillators are chaotic or have a variable period as a result of interaction with the other oscillators, the interaction having the effect of constantly pulling the populations away from their natural attractors.

From the set of frequencies we calculate the relative standard deviation

$$\sigma = \frac{\text{standard deviation}(\omega_{i,j})}{\text{mean}(\omega_{i,j})} \times 100.$$

The peak times data are used to calculate phase information for each population. We linearly interpolate between peaks so that the phase at time t is

$$\theta_{i,j}(t) = \left(\frac{t - T_m}{T_{m+1} - T_m}\right)2\pi,$$

where T_m and T_{m+1} are the peaks in $P_{i,j}$ occurring before and after t.

Given the phase $\theta_{i,j}$ of each oscillator, we then calculate the centroid of the oscillators positions on the circle

$$Z = R\,\mathrm{e}^{\imath\psi} = \frac{1}{n^2}\sum_{i=1}^{n}\sum_{j=1}^{n}\mathrm{e}^{\imath\theta_{ij}},$$

so that ψ gives the average phase and the *order parameter* R is a measure of the phase coherence of the ensemble.

For each time-step, the cluster measure $c(t)$ is calculated by taking the $n \times n$ $P_{i,j}$ field

$$\mathbf{P}(t) = \begin{pmatrix} P_{1,1} & P_{1,2} & \cdots & P_{1,n} \\ P_{2,1} & \cdots & \cdots & P_{1,n} \\ \vdots & & & \\ P_{n,1} & P_{n,2} & \cdots & P_{n,n} \end{pmatrix},$$

and removing its mean to obtain

$$\bar{\mathbf{P}}(t) = \mathbf{P}(t) - \mathrm{mean}(\mathbf{P}(t)).$$

We look at the size of structure in the x and y directions separately to obtain measures c_x and c_y. For c_x we take a transect

$$\bar{P_i} = (\bar{P_{i1}}, \bar{P_{i2}}, \ldots, \bar{P_{in}}),$$

across the lattice for each of the $i = 1, \ldots, n$ rows of grid-cells of the mean-removed field. Clusters are defined as regions of adjacent grid-cells with continuously positive or negative values and their boundaries are found by recording zero-crossings of P_i. Over all rows, this gives a set of clusters

$$\mathrm{clusters}_x = \{c_1, c_2, \ldots, c_m\},$$

where c_k, for $k = 1, \ldots, m$, are integer numbers of grid-cells forming each cluster and $\sum_{k=1}^{m}(c_k) = n^2$. The median of this set of clusters is then calculated for each time-step to give a measure of the local coherency $c_x(t)$, which can also be averaged over time. $c_y(t)$ is calculated in exactly the same manner, but using columns rather than rows of $\bar{\mathbf{P}}(t)$. The cluster measure given here is only well-defined when clusters exist. That is, it has meaning when there exist well-defined synchronised regions separated by sharp transitions. In this case, c is a good representation of the size, in grid-cells, of these clusters. If such clusters do not exist, and we have instead a gradual shift in phytoplankton biomass values from grid-cell to grid-cell, then the cluster measure as defined here is not appropriate. Take the simple example of a frequency-locked but not phase-locked ensemble with a linear increase in phytoplankton biomass from the left-hand edge to the right-hand edge of the lattice; removing the mean and calculating c in this example will give $c = \frac{n}{2}$, apparently indicating a representative cluster size of half the lattice, whereas actually a cluster size of n is more meaningful since no sharp transitions exist. Additionally, for large cluster sizes with respect to the domain size, the c measure will be inherently less reliable than for small clustering: fewer larger clusters will fit into the domain, reducing the probability when taking the median of obtaining an accurate estimate for c. For this reason, in conjunction with the cluster measure we also consider a measure of the sharpness of transitions from grid-cell to grid-cell across the lattice to show the sharp edges of clusters and to highlight where c is less appropriate. For each time-step we normalise the $\mathbf{P}(t)$ field to obtain

$$\hat{\mathbf{P}}(t) = \left(\frac{\mathbf{P}(t) - \min(P_{i,j}(t))}{\max(\mathbf{P}(t) - \min(P_{i,j}(t)))}\right),$$

with $0 \leqslant \hat{P}_{i,j}(t) \leqslant 1$ for $i,j = 1, \ldots, n$. For each grid-cell, we define $g_{i,j}(t)$ as the maximum value of the absolute difference between $\hat{P}_{i,j}(t)$ and the phytoplankton biomass in each of its up to eight (for interior populations) nearest neighbours, i.e. for interior populations,

$$g_{i,j}(t) = \max\{|\hat{P}_{i,j} - \hat{P}_{i',j'}|\},$$

for $i' = i-1, i, i+1$ and $j' = j-1, j, j+1$. Then,

$$g(t) = \max_{i,j}(g_{i,j}(t)).$$

References

Abraham, E., 1998. The generation of plankton patchiness by turbulent stirring. Nature 391, 577–580.

Alpine, E., Cloern, J.E., 1988. Phytoplankton growth rates in a light limited environment, San Francisco Bay. Marine Ecology Progress Series 44, 167–173.

Bainbridge, R., 1956. The size, shape and density of marine phytoplankton concentrations. Biology Review 32, 91–115.

Barbay, Giacomelli, G., Marin, F., 2000. Stochastic resonance in vertical cavity surface emitting lasers. Physical Review E 61 (1), 157–166.

Belykh, I., Belykh, V., Nevidin, K., Hasler, M., 2003. Persistent clusters in lattices of coupled nonidentical chaotic systems. Chaos 13 (1), 165–178.

Benton, T.G., Lapsley, C.T., Beckerman, A.P., 2001. Population synchrony and environmental variation: an experimental demonstration. Ecology Letters 4, 236–243.

Blasius, B., Montbrió, E., 2003. Anomalous phase synchronisation in populations of nonidentical oscillators. Physical Review E 67.

Blasius, B., Tönjes, R., 2005. Quasiregular concentric waves in heterogeneous lattices of coupled oscillators. Physical Review Letters 95, 084101.

Blasius, B., Huppert, A., Stone, L., 1999. Complex dynamics and phase synchronization in spatially extended ecological systems. Nature 399, 354–359.

Boccaletti, S. (Ed.), 2002. Complex Synchronization Phenomena in Ecological Systems, vol. 6 of Experimental Chaos. American Institute of Physics.

Edwards, A.M., 2001. Adding detritus to a nutrient–phytoplankton–zooplankton model: a dynamical systems approach. Journal of Plankton Research 23 (4), 389–413.

Edwards, A.M., Brindley, J., 1996. Oscillatory behaviour in a three-component plankton population model. Dynamics and Stability of Systems 11 (4), 347–370.

Elton, C., Nicholson, M., 1942. The ten-year cycle in numbers of the lynx in Canada. Journal of Animal Ecology 11 (2), 215–244.

Eppley, R.W., 1972. Temperature and phytoplankton growth in the sea. Fisheries Bulletin 70, 1063–1085.

Fasham, M.J.R. (Ed.), 2003. Ocean Biogeochemistry. The IGBP Series: Global Change. Springer.

Fussman, G.F., Ellner, S.P., Shertzer, K.W., Hairston Jr, N.G., 2000. Crossing the Hopf bifurcation in a live predator–prey system. Science 290 (5495), 1358–1360.

Grenfall, B.T., Wilson, K., Finkenstadt, B.F., Coulson, T.N., Murray, S., Albon, S.D., Pemberton, J.M., Clutton-Brock, T.H., Crawley, M.J., 1998. Noise and determinism in synchronised sheep dynamics. Nature 394, 673–677.

Guirey, E.J., 2007. Application of synchronisation theory to plankton patchiness. Ph.D. Thesis. School of Ocean and Earth Sciences, University of Southampton.

Guirey, E.J., Bees, M.A., Martin, A.P., Srokosz, M.A., Fasham, M.J.R., 2007. Emergent features due to grid-cell biology: synchronisation in biophysical models. Bulletin of Mathematical Biology 69 (4), 1401–1422.

Haydon, D.T., Stenseth, N.C., Boyce, M.S., Greenwood, P.E., 2001. Phase coupling and synchrony in the spatiotemporal dynamics of muskrat and mink populations across Canada. Ecology 98 (23), 13149–13154.

Hillary, R.M., Bees, M.A., 2004a. Plankton lattices and the role of chaos in plankton patchiness. Physical Review E 69 (031913).

Hillary, R.M., Bees, M.A., 2004b. Synchrony and chaos in patchy ecosystems. Bulletin of Mathematical Biology 66, 1909–1931.

Holyoak, M., Lawler, S.P., 1996. Persistence of an extinction-prone predator prey interaction through metapopulation dynamics. Ecology 77 (6), 1867–1879.

Levy, M., Klein, P., 2004. Does the low frequency variability of mesoscale dynamics explain a part of the phytoplankton and zooplankton spectral variability? Proceedings of the Royal Society of London A 460, 1673–1687.

Martin, A.P., Srokosz, M.A., 2002. Plankton distribution spectra: inter-size class variability and the relative slopes for phytoplankton and zooplankton. Geophysical Research Letters 29 (24), 2213–2216.

Moran, P.A.P., 1953. The statistical analysis of the Canadian lynx cycle. Australian Journal of Zoology 1, 291–298.

Néda, Z., Ravasz, E., Brechet, Y., Vicsek, T., Barabssi, A.L., 2000. Tumultuous applause can transform itself into waves of synchronized clapping. Nature 403, 157–166. 849–850.

Neff, J., Carroll, T.L., 1993. Circuits that get chaos in sync. Scientific American 296, 101–103.

Okubo, A., 1971. Oceanic diffusion diagrams. Deep-Sea Research 18, 789–802.

Osipov, G.V., Sushchik, M.M., 1997. The effect of natural frequency distribution on cluster synchronization in oscillator arrays. IEEE Transactions on Circuits an Systems I: Fundamental Theory and Applications 44 (10), 1006–1010.

Pascual, M., Roy, M., Guichard, F., Flierl, G., 2002. Cluster size distributions: signatures of self-organization in spatial ecologies. Philosophical Transactions of the Royal Society of London B 357, 657–666.

Pikovsky, A., Michael, R., Kurths, J., 2001. Synchronisation: A Universal Concept in Nonlinear Sciences. Cambridge Nonlinear Science Series. Cambridge University Press, Cambridge.
Ranta, E., Kaitala, V., Lindstrom, J., Linden, H., 1995. Synchrony in population dynamics. Proceedings of the Royal Society of London B 262, 113–118.
Ryabchenko, V.A., Fasham, M.J.R., Kagan, B.A., Popova, E.E., 1997. What causes short-term oscillations in ecosystem models of the ocean mixed layer? Journal of Marine Systems 13, 33–50.
Sherratt, T.N., Lambin, X., Petty, S.J., Mackinnon, J.L., Coles, C.F., Thomas, C.J., 2000. Use of coupled oscillator models to understand synchrony and travelling waves in populations of the field vole *Microtus agrestis* in northern England. Journal of Applied Ecology 37, 148–158.
Steele, J.H., 1974. Spatial heterogeneity and population stability. Nature 248, 83.
Steele, J.H. (Ed.), 1978. Spatial Pattern in Plankton Communities. Plenum Press.
Steele, J.H., Henderson, E.W., 1981. A simple plankton model. The American Naturalist 344, 734–741.
Steele, J.H., Henderson, E.W., 1992. A simple model for plankton patchiness. Journal of Plankton Research 14 (10), 1397–1403.
Strogatz, S.H., Stewart, I., 1993. Coupled oscillators and biological synchronisation. Scientific American 269, 68–75.
Taherion, S., Lai, Y.C., 1999. Observability of lag synchronization of coupling chaotic oscillators. Physical Review E 59 (6), 6247–6250.
Totterdell, I.J., 1993. An annotated bibliography of marine biological models. In: Evans, G.T., Fasham, M.J.R. (Eds.), Towards a Model of Ocean Biogeochemical Processes, vol. 10. NATO.
Tzella, A., Haynes, P.H., 2007. Small-scale spatial structure in plankton distributions. Biogeosciences 4, 173–179.
Ydenberg, R.C., 1987. Nomadic predators and geographical synchrony in microtine population cycles. OIKOS 50 (2), 270–272.
Ylikarjula, J., Alaja, S., Laaksos, J., Tesar, D., 2000. Effects of patch number and dispersal patterns on population dynamics and synchrony. Journal of Theoretical Biology 207, 377–387.